IAI Journals.ASM.org

Mycoplasma pneumoniae Modulates STAT3-STAT6/EGFR-FOXA2 Signaling To Induce Overexpression of Airway Mucins

Yonghua Hao,[a] Zhizhou Kuang,[a] Jia Jing,[a] Jinfeng Miao,[b] Li Yu Mei,[a] Ryan J. Lee,[a] Susie Kim,[a] Shawn Choe,[a] Duncan C. Krause,[c] Gee W. Lau[a]

Department of Pathobiology, University of Illinois at Urbana-Champaign, Urbana, Illinois, USA[a]; College of Veterinary Medicine, Nanjing Agricultural University, Nanjing, People's Republic of China[b]; Department of Microbiology, University of Georgia, Athens, Georgia, USA[c]

Aberrant mucin secretion and accumulation in the airway lumen are clinical hallmarks associated with various lung diseases such as asthma, chronic obstructive pulmonary disease, and cystic fibrosis. *Mycoplasma pneumoniae*, long appreciated as one of the triggers of acute exacerbations of chronic pulmonary diseases, has recently been reported to promote excessive mucus secretion. However, the mechanism of mucin overproduction induced by *M. pneumoniae* remains unclear. This study aimed to determine the mechanism by which *M. pneumoniae* induces mucus hypersecretion by using *M. pneumoniae* infection of mouse lungs, human primary bronchial epithelial (NHBE) cells cultured at the air-liquid interface, and the conventionally cultured airway epithelial NCI-H292 cell line. We demonstrated that *M. pneumoniae* induced the expression of mucins MUC5AC and MUC5B by activating the STAT6-STAT3 and epidermal growth factor receptor (EGFR) signal pathways, which in turn downregulated FOXA2, a transcriptional repressor of mucin biosynthesis. The upstream stimuli of these pathways, including interleukin-4 (IL-4), IL-6, and IL-13, increased dramatically upon exposure to *M. pneumoniae*. Inhibition of the STAT6, STAT3, and EGFR signaling pathways significantly restored the expression of FOXA2 and attenuated the expression of airway mucins MUC5AC and MUC5B. Collectively, these studies demonstrated that *M. pneumoniae* induces airway mucus hypersecretion by modulating the STAT/EGFR-FOXA2 signaling pathways.

Airway mucus forms a protective coating that entraps foreign particles and microbes, facilitating their clearance by mucociliary transport. Mucus is composed mainly of mucin glycoproteins, water, ions, and cellular debris. Mucins are the major macromolecular component of the mucus gel responsible for its viscoelastic, rheological, and clearance properties. MUC5AC and MUC5B are the major mucins of human airways (1–3). Although a deficient mucous barrier intuitively leaves the lungs vulnerable to injury, aberrant mucin secretion and accumulation contribute significantly to the pathogenesis of airway diseases such as asthma, chronic obstructive pulmonary disease (COPD), and cystic fibrosis (CF) (1–4). Mucus plugging in asthmatic and COPD lungs is a major cause of airway narrowing and death (5, 6). Furthermore, hypersecretion of MUC5AC is detrimental during acute lung injury (7).

The ability of microbial pathogens to induce mucus secretion suggests that it is one of the mechanisms of infection-induced exacerbation in airway diseases (8–11). *M. pneumoniae* is the most common cause of community-acquired pneumonia. Moreover, *M. pneumoniae* has long been recognized as a trigger of both chronic infection and acute exacerbation in multiple chronic airway diseases, including asthma (12, 13). Several virulence mechanisms of *M. pneumoniae* are known, including cytoadherence through a polar attachment organelle (14), generation of reactive oxygen species (ROS) (15), and secretion of the community-acquired respiratory distress syndrome (CARDS) toxin (16). Although *M. pneumoniae* and CARDS toxin induce mucin expression (9, 10, 17), the signal pathways within the airway epithelium that regulate the response to *M. pneumoniae* remain unknown. Previously, we have shown that *Pseudomonas aeruginosa* induces goblet cell hyperplasia and metaplasia (GCHM) and mucus hypersecretion by secreting the redox-active toxin pyocyanin, which induces STAT6 and epidermal growth factor receptor (EGFR) signaling to inactivate FOXA2, a major transcriptional repressor of GCHM and mucin biosynthesis (18, 19). Pyocyanin also redox inactivates FOXA2 through posttranslational modifications, resulting in the overexpression of mucins (20). Importantly, the expression of FOXA2 is depleted in the airways of bronchiectatic and asthmatic patients, as well as in the ovalbumin-induced mouse model of asthma (19, 21). In this study, we examined the airway signaling mechanisms modulated by *M. pneumoniae* that resulted in FOXA2 depletion and overexpression of mucins.

MATERIALS AND METHODS

***M. pneumoniae* preparation.** *M. pneumoniae* strain M129 was cultured in SP-4 broth medium at 37°C until the color of the medium changed to peach yellow. *M. pneumoniae* cells were dislodged with a dish scraper and suspended in sterile saline. The *M. pneumoniae* mixture was passed through a 25-gauge needle 10 times. The stock was stored at −80°C. A portion of the stock was serially diluted and plated onto pleuropneumonia-like organism (PPLO) blood agar to determine the CFU count as previously described (22). *M. pneumoniae* M129 grew slowly, yielding extremely small colonies on PPLO blood agar after 7 days at 37°C. Plates were then overlaid with blood agar, and 2 days later, colonies were visible

Received 28 April 2014 Returned for modification 2 June 2014
Accepted 26 September 2014
Published ahead of print 6 October 2014
Editor: B. A. McCormick
Address correspondence to Gee W. Lau, geelau@illinois.edu.
Y.H. and Z.K. contributed equally to this work.
Supplemental material for this article may be found at http://dx.doi.org/10.1128/IAI.01989-14.

doi:10.1128/IAI.01989-14

as hemolytic plaques. The original stock was diluted to 1×10^8 cells/50-μl aliquot and stored at −80°C. All subsequent experiments were performed with aliquots of same frozen stock preparation.

Mouse handling and exposure to *M. pneumoniae*. Six-week-old wild-type C57BL/6 mice (Harlan Sprague Dawley) and isogenic Stat6$^{-/-}$ mice (Jackson Laboratory) were housed in positively ventilated microisolator cages with automatic recirculating water that were located in a room with laminar, high-efficiency particle accumulation-filtered air. The animals received autoclaved food, water, and bedding. Isoflurane-anesthetized mice (groups of 12 to 20) were intranasally infected with *M. pneumoniae* M129 (1×10^8 CFU in 50 μl) on day 0. Control mice were exposed to 50 μl of phosphate-buffered saline (PBS). On day 3, mouse lungs were collected for analyses. These animal studies were carried out in strict accordance with the Guide for the Care and Use of Laboratory Animals of the National Institutes of Health. The protocol was approved by the Institutional Animal Care and Use Committee at the University of Illinois at Urbana-Champaign.

Cytokine analyses. The levels of interleukin-4 (IL-4), IL-6, and IL-13 in the bronchoalveolar lavage (BAL) fluid of mouse lungs were determined with specific enzyme-linked immunosorbent assay (ELISA) kits according to the manufacturer's protocols (R&D Systems) and by immunohistochemistry (IHC) analysis.

Histopathology and IHC analyses. Mouse lungs were processed as described previously (18, 20). Briefly, a cannula was inserted into the trachea and the lungs were instilled with 10% neutral buffered formalin at a constant pressure (25 cm H_2O). The inflated lungs were fixed for 24 h, embedded in paraffin wax, and sectioned. Paraffin-embedded sections (~5-μm thickness) were stained with periodic acid-Schiff (PAS) reagent. For IHC analyses, lung sections were stained with primary antibodies and visualized with the ABC kit (Vector Labs). Quantitative analyses of lung tissues stained with PAS and various antibodies were performed with AxioVision release 4.8 software (Carl Zeiss).

Antibodies. The primary monoclonal and polyclonal antibodies used and their dilutions for use in Western blotting (WB), IHC, and immunofluorescence (IF) assays are described below. Antibodies to the following were purchased from Santa Cruz Biotechnology: IL-4 (sc-73318; dilution for IHC, 1:100), IL-13 (sc-1776; dilution for IHC, 1:100), MUC5AC (sc-71620; dilution for WB, 1:500; dilution for IHC, 1:100; dilution for IF assays, 1:200), MUC5B (sc-20119; dilution for WB, 1:500; dilution for IHC, 1:200; dilution for IF assays, 1:100), FOXA2 (sc-101060; dilution for WB, 1:1,000; dilution for IHC, 1:500), EGFR (sc-03; dilution for WB, 1:500), p-EGFR (sc-101668; dilution for WB, 1:500), and H3 (sc-10809; dilution for WB, 1:1,000). Antibodies to the following were purchased from Cell Signaling Technology: p-STAT3 (4113; dilution for WB, 1:1,000), p-STAT6 (9361; dilution for WB, 1:1,000), and glyceraldehyde 3-phosphate dehydrogenase (GAPDH) (2118; dilution for WB, 1:1,000). Antibodies to the following were purchased from Abcam: IL-6 (ab6672; dilution for WB, 1:500; dilution for IHC, 1:500), STAT3 (ab5073; dilution for WB, 1:1,000), and STAT6 (ab44718; dilution for WB, 1:1,000).

Cell cultures. The human lung mucoepidermoid carcinoma cell line NCI-H292 was purchased from the American Type Culture Collection (ATCC; Manassas, VA). NCI-H292 cells were cultured in RPMI 1640 medium supplemented with 10% fetal bovine serum (Sigma) in a 5% CO_2 incubator. After reaching 70% confluence, cells were serum starved for 24 h to synchronize the cell cycle and to return various signaling pathways potentially activated by serum to basal levels before exposure to *M. pneumoniae* at the indicated multiplicity of infection (MOI) or to various inhibitors or transfection with small interfering RNA (siRNA). Control cells were exposed to sterile PBS.

Normal human bronchial epithelial (NHBE) cells were purchased from Lonza (Walkersville, MD) and cultured as we have previously described (18, 20). Cells were thawed and passaged in 5% CO_2 at 37°C with bronchial epithelial growth medium (BEGM) supplemented with growth factors supplied in the SingleQuot kit (Lonza). Cells at passage 3 were trypsinized and seeded onto Costar Transwell inserts with a 0.4-μm pore size (Corning) at a density of $1.5 \times 10^5/cm^2$ in medium composed of 50% bronchial epithelial basal medium and low-glucose 50% Dulbecco's modified Eagle's medium-F12 (Invitrogen) supplemented with the growth factors provided in the SingleQuot kits and retinoic acid (50 nM). Once the cells reached confluence (approximately 7 days after seeding, as determined by transepithelial electrical resistance measurements [data not shown]), they were switched to an air-liquid interface (ALI) for an additional 2 weeks to achieve mucociliary differentiation. NHBE cells were infected with *M. pneumoniae* M129 (MOI, 50:1), stained with anti-MUC5AC and anti-MUC5B antibodies, and visualized with an Alexa Fluor 647-conjugated secondary antibody (red color) and an Alexa Fluor 488-conjugated secondary antibody (green color) under a confocal microscope, respectively. Nuclei were stained with 4′,6-diamidino-2-phenylindole (DAPI) (blue color). The percentage of MUC5AC or MUC5B expression was calculated on the basis of the fluorescence signal of MUC5AC or MUC5B divided by the total DAPI signal (blue). Fluorescence signals were quantified with the AxioVision release 4.8 software.

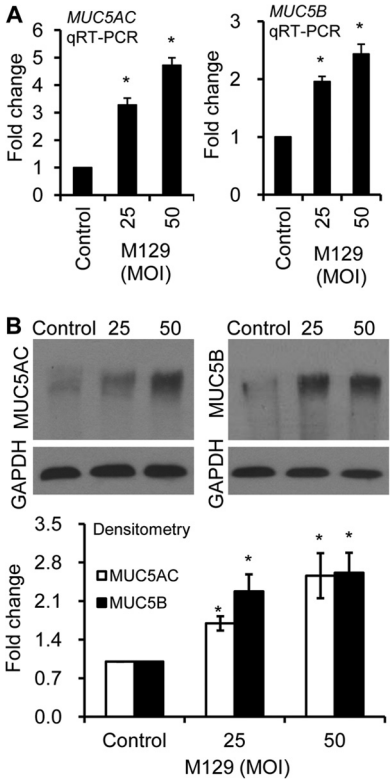

FIG 1 *M. pneumoniae* induces the expression of MUC5AC and MUC5B in NCI-H292 cells. (A) After an 18-h incubation with the indicated MOI of *M. pneumoniae* M129, *MUC5AC* and *MUC5B* mRNA levels were determined by qRT-PCR. (B) Mucins levels were determined by Western blotting and quantified by densitometry. The qRT-PCR was performed in triplicate in three independent experiments. Western blotting experiments were repeated three times with similar results. Data for qRT-PCR and densitometry of Western blot assays represent the means ± the standard deviations from all three experiments. *, $P < 0.05$ for comparison of *M. pneumoniae*-infected samples with PBS controls. The statistical significance of differences between samples in both panels A and B was determined by one-way ANOVA.

qRT-PCR. NCI-H292 cells were exposed to *M. pneumoniae* M129 at the indicated MOI for 18 h. Total RNA was extracted with the RNeasy minikit (Qiagen). Equal amounts of total RNA (3 μg) were reverse transcribed into cDNA with oligo(dT) primers and SuperScript III reverse transcriptase (Invitrogen). The first-strand cDNA was then diluted and used in each subsequent PCR. For quantitative real-time PCR (qRT-PCR), 10 μl of cDNA was used with 6-carboxyfluorescein-labeled

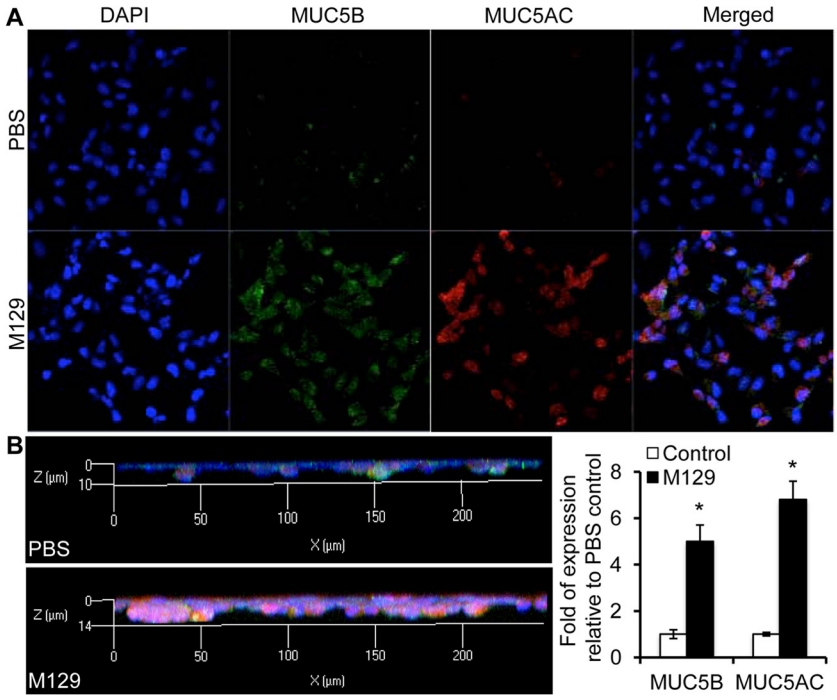

FIG 2 *M. pneumoniae* induced the expression of MUC5AC and MUC5B in ALI cultures of NHBE cells. Differentiated NHBE cells were exposed to PBS or *M. pneumoniae* M129 (MOI of 50:1) for 18 h. Mucins MUC5B and MUC5AC were stained with specific primary antibodies and visualized with an Alexa Fluor 488-conjugated secondary antibody (green, MUC5B) or an Alexa Fluor 647-conjugated secondary antibody (red, MUC5AC). Nuclei were stained with DAPI (blue). (A) Top-down images of stained cells. (B) Z-stack images of stained cells. Three independent experiments showed similar results. Typical strips of cells are shown. The expression of MUC5B and MUC5AC from 10 representative strips was quantified with the AxioVision release 4.8 software. The statistical significance of differences between samples was determined with the parametric Student *t* test.

TaqMan primers predesigned by Applied Biosystems on the basis of the detected gene sequence and a 7900 HT real-time PCR system (Applied Biosystems) according to the manufacturer's protocol. The relative expression of the *MUC5AC* and *MUC5B* genes was normalized to that of the gene for GAPDH. The sequences of the primers used can be obtained from Applied Biosystems under identification numbers Hs01370716_m1, Hs 00861588_m1, and Hs 99999905_m1, respectively.

Western blotting analyses. Western blot assays were performed with total, nuclear (for FOXA2), or crude plasma membrane (for EGFR) proteins of *M. pneumoniae* M129 or PBS-exposed NCI-292 cells after lysis by the ProteoJET Mammalian Cell Lysis Reagent (Fermentas) (18). Equal amounts of total protein per sample were separated by SDS-PAGE (8% polyacrylamide) and transferred to polyvinylidene difluoride membranes (Bio-Rad). Membranes were probed with the individual antibodies described above. The immune complexes were visualized with the ECL Western blotting detection system (Amersham Biosciences) and Kodak BIOMAX (Kodak) X-ray film.

ROS assays. ROS levels in *M. pneumoniae*-infected (18 h) NCI-H292 cells were determined with the OxiSelect In Vitro ROS/RNS assay kit according to the manufacturer's protocols (Cell Biolabs).

Inhibitor studies. After reaching 70% confluence, NCI-H292 cells were serum starved for 24 h and exposed to the indicated concentration of the STAT6 inhibitor kaempferol (TOCRIS Bioscience), the STAT3 inhibitor IX Cpd188 (Calbiochem), or the EGFR inhibitor AG1478 (Calbiochem). After 90 min, cells were exposed to the indicated MOI of *M. pneumoniae* M129 or PBS for 18 h. The amount of FOXA2 within the nuclei of NCI-H292 cells was determined with the anti-FOXA2 antibody.

siRNA studies. siRNAs against EGFR (6480S), STAT3 (6580S), and STAT6 (6358S) and the random, nontargeting siRNA sequence (SignalSilence Control siRNA, unconjugated, 6568S, 6201S) were purchased from Cell Signaling Technology. Serum-starved NCI-H292 cells were transfected with each siRNA at 100 nM with the Lipofectamine RNAiMAX Transfection Reagent (Life Technologies 13778150) according to the manufacturer's protocols. After 48 h, transfected cells were infected with *M. pneumoniae* M129 for 18 h at an MOI of 25. FOXA2 expression in these NCI-H292 cells was analyzed as described above.

Statistical analysis. Quantitative data were expressed as mean values ± standard errors. The statistical significance of differences between samples with equal variances were determined with the parametric Student *t* test for two unpaired samples. For comparison of the means of groups of three or more, data were analyzed for statistical significance by analysis of variance (ANOVA), followed by Tukey's test for comparison of the means. A significant difference was considered to be a P value of <0.05.

RESULTS

***M. pneumoniae* induces the expression of mucins in NCI-H292 cells.** Mucin production is increased during pulmonary exacerbation in asthma, CF, and COPD patients (1–6). We examined the induction of the *MUC5AC* and *MUC5B* genes by *M. pneumoniae* in NCI-H292 cells. At MOIs of both 25:1 and 50:1, *M. pneumoniae* M129 induced significantly higher transcription of the *MUC5AC* and *MUC5B* genes (Fig. 1A), as well as the expression of both mucins, as determined by Western blot assays and densitometry (Fig. 1B).

***M. pneumoniae* induces the expression of mucins in primary human bronchial epithelial cells cultured at the ALI.** Airway epithelial cells grown in ALI culture have emerged as a powerful tool for the study of airway biology. For example, we have shown that *P. aeruginosa* pyocyanin induces ALI cultures of NHBE cells to secrete MUC5AC and MUC5B, major mucins found in healthy

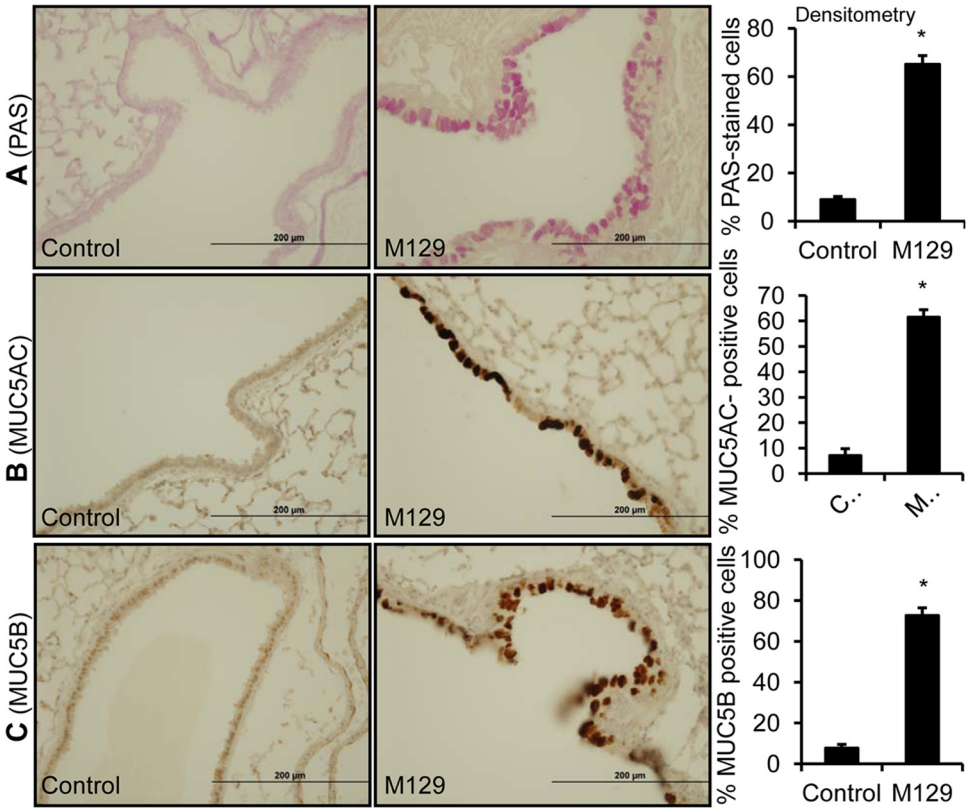

FIG 3 Exposure to *M. pneumoniae* induces hypersecretion of MUC5AC and MUC5B in mouse airways. Lung sections from control PBS-treated or *M. pneumoniae*-infected C57BL/6 mice ($n = 12$ to 20) were stained with PAS (A) or with a 3,3′-diaminobenzidine staining kit with an anti-MUC5AC (B) or anti-MUC5B primary antibody (C). The conducting airways of control mice showed low or barely detectable numbers of goblet cells with basal levels of MUC5AC and MUC5B (A). *M. pneumoniae*-infected conducting airways showed GCHM with expression of MUC5AC (B) and MUC5B (C). Semiquantitative analysis of mucin-positive cells from 10 mouse lungs were performed with the AxioVision release 4.8 software. *, $P < 0.05$ for comparison of *M. pneumoniae*-infected samples with PBS controls. The statistical significance of differences between samples was determined with the parametric Student *t* test.

and diseased human airways (18, 20). We examined if *M. pneumoniae* M129 could induce the expression of MUC5AC and MUC5B in an ALI culture of NHBE cells. Control NHBE cells exposed to PBS expressed basal levels of mucins (Fig. 2A and B). In contrast, after 18 h of infection with *M. pneumoniae* M129, NHBE cells expressed 6.8- and 5-fold more of the mucins MUC5AC and MUC5B, respectively (Fig. 2A and B). Collectively, these results indicate that *M. pneumoniae* M129 induces MUC5AC and MUC5B expression in ALI cultures of airway epithelial cells.

***M. pneumoniae* upregulates the expression of mucins in mouse airways.** We further confirmed the ability of *M. pneumoniae* to induce the expression of MUC5AC and MUC5B in mice. Mouse lungs exposed to PBS remained normal, with few mucin-positive goblet cells and trace amounts of MUC5AC and MUC5B (Fig. 3A). In contrast, after 3 days of infection with *M. pneumoniae* M129, the conducting airways of mice developed GCHM and mucus hypersecretion (Fig. 3A) and significantly higher expression of the mucins MUC5AC (8.8-fold, Fig. 3B) and MUC5B (9.4-fold, Fig. 3C). Together, both the *in vivo* and *in vitro* data indicate that *M. pneumoniae* induces GCHM and mucin hypersecretion in airways.

***M. pneumoniae* inhibits the expression of FOXA2.** FOXA2 is a transcriptional repressor of GCHM and mucin biosynthesis. The lungs of Foxa2$^{-/-}$ mice develop airspace enlargement, GCHM, increased mucin production, and neutrophilic infiltration (19). Analysis of lung tissues from patients with bronchopulmonary dysplasia and bronchiectasis (19) and asthma (21) reveals a strong inverse correlation between FOXA2 and GCHM protein levels. Because *M. pneumoniae* infection induces the overexpression of MUC5AC and MUC5B, we hypothesized that it impaired the expression of FOXA2. *M. pneumoniae* M129 induced dose-dependent 38% (MOI of 25), 51% (MOI of 50), and 74% (MOI of 100) inhibition, respectively, of FOXA2 expression in NCI-H292 cells (Fig. 4A). Similarly, FOXA2 expression was significantly attenuated in mouse airways infected with *M. pneumoniae* M129 (Fig. 4B). The conducting airways of PBS-exposed mice showed strong expression of FOXA2 in the nuclei of epithelial cells lining the large bronchi (Fig. 4B, left). In contrast, the expression of FOXA2 within the nuclei of goblet cells in *M. pneumoniae* M129-infected airways was severely depleted (Fig. 4B, middle). Semiquantitative analysis with the AxioVision release 4.8 software indicated that the total number of FOXA2-positive cells was 86% lower in *M. pneumoniae* M129-infected airways than in control airways (Fig. 4B, right). Collectively, our *in vitro* and *in vivo* experimental results suggest that *M. pneumoniae* causes mucin hypersecretion by suppressing the expression of FOXA2.

***M. pneumoniae* activates STAT3-STAT6 signaling pathways.** The IL-4/IL-13–STAT6 signaling pathway has been shown to induce the expression of mucins (1, 3), in part by inhibiting the expression of FOXA2 (18, 19, 23). Similarly, the IL-6–STAT3

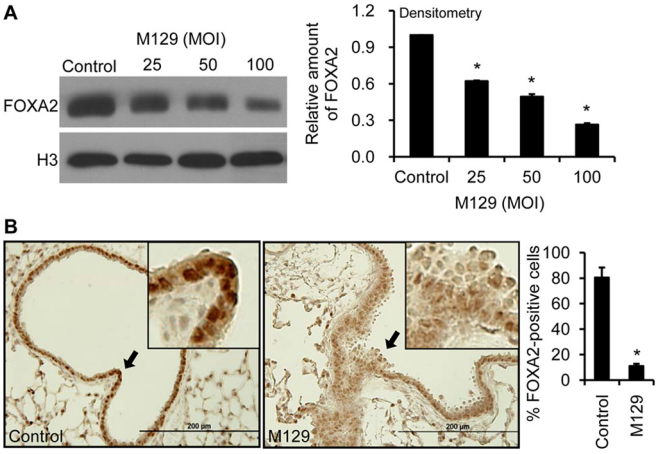

FIG 4 Exposure to *M. pneumoniae* inhibits FOXA2 expression. (A) Western blotting and densitometry of FOXA2 in NCI-H292 cells 18 h after exposure to PBS or *M. pneumoniae* M129 at the indicated MOI. Western blotting experiments were repeated three times with similar results. Densitometry of Western blot assays represents the mean ± the standard deviation from all three experiments. The statistical significance of differences between the densitometry of Western blot assays was determined by one-way ANOVA. (B) Lung sections of C57BL/6 mice after 3 days of exposure to PBS (control) or 1×10^8 CFU of *M. pneumoniae* M129. Tissues were stained with anti-FOXA2 primary antibodies and visualized with the ABC kit. FOXA2-positive cells from 10 mouse lungs were quantified with the AxioVision release 4.8 software. *, $P < 0.05$ for comparison of *M. pneumoniae*-infected samples with PBS controls. The statistical significance of differences between samples was determined with the parametric Student *t* test.

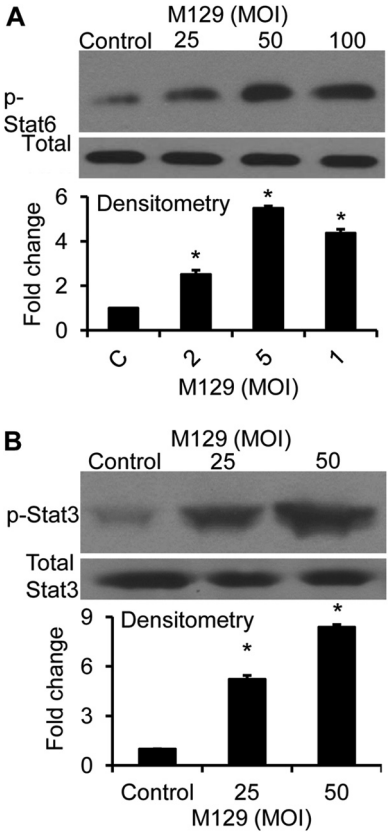

FIG 5 *M. pneumoniae* infection activates the progoblet cell hyperplasia and metaplasia STAT3 and STAT6 signaling pathways. After 18 h of exposure to *M. pneumoniae* or PBS, phosphorylated STAT6 (A) and STAT3 (B) were detected in NCI-H292 cells with specific anti-phospho antibodies. Western blotting experiments were repeated three times with similar results. Densitometry of Western blot assays represents the mean values ± the standard deviations from all three experiments. *, $P < 0.05$ for comparison of *M. pneumoniae*-infected samples with PBS controls. The statistical significance of differences between densitometry of Western blot assays in both panels A and B was determined by one-way ANOVA.

pathway plays a role in a murine model of asthma mediated by dust mites (24). STAT3 is also activated through ROS released during exposure to lipid-associated membrane proteins from *M. pneumoniae* (25). Thus, we examined the activation of STAT6 and STAT3 by *M. pneumoniae* M129 in NCI-H292 cells. Western blot analysis indicated that at an MOI of 50, the amounts of phosphorylated STAT6 (Fig. 5A) and STAT3 (Fig. 5B) were significantly elevated 5.5- and 8.4-fold, respectively, when cells were exposed to increasing concentrations of *M. pneumoniae* M129. Consistent with the data in Fig. 5, exposure to *M. pneumoniae* M129 but not PBS significantly increased the levels of upstream Th2 cytokines IL-4 and IL-13, which activate STAT6 (2.2- and 3.6-fold, respectively, Fig. 6A and B), and IL-6, which activates STAT3 (2.6-fold, Fig. 6C) in mouse lungs. In contrast, the levels of IL-4, IL-13, and IL-6 were indistinguishable in the lungs of Stat6$^{-/-}$ mice exposed to PBS or *M. pneumoniae* M129. IHC analyses (arrows) of mouse lungs further confirmed the ELISA results (Fig. 6A to C). Collectively, both *in vitro* and *in vivo* results indicate that *M. pneumoniae* infection activates STAT3 and STAT6. Because the level of IL-6 is not upregulated in Stat6$^{-/-}$ mice, this suggests that IL-6-activated STAT3 may function within the STAT6 signaling pathway in response to *M. pneumoniae* infection.

***M. pneumoniae* activates EGFR signaling.** The EGFR signaling pathway also activates mucin expression, partially through induction by ROS (3, 18, 26). Activation of EGFR inhibits FOXA2 expression (18, 23). The ability of *M. pneumoniae* to induce ROS production in airway epithelial cells is an important virulence mechanism (27). We confirmed that *M. pneumoniae* M129 infection was accompanied by a dose-dependent increase in ROS formation (Fig. 7A), as well as increased levels of phosphorylated EGFR, in NCI-H292 cells (Fig. 7B). Addition of glutathione (GSH) attenuated EGFR activation, with corresponding restoration of FOXA2 expression (Fig. 7C). Interestingly, even though ROS was reported to induce STAT3 during exposure to lipid-associated membrane proteins of *M. pneumoniae* (24), GSH did not attenuate the ability of live *M. pneumoniae* M129 bacterial cells to activate STAT3 (Fig. 7C). Together, these results indicate that *M. pneumoniae* activates pro-GCHM and mucin biosynthesis signaling pathways to inhibit FOXA2 expression.

Inhibition of STAT3, STAT6, and EGFR signaling pathways attenuates FOXA2 repression and mucin overproduction mediated by *M. pneumoniae*. To confirm that *M. pneumoniae* inhibits the expression of FOXA2 by activating STAT3, STAT6, and EGFR signaling pathways, we examined the ability of the STAT3 inhibitor IX Cpd188, the STAT6 inhibitor kaempferol, and the EGFR inhibitor AG1478, respectively, to relieve repression of FOXA2. Because a STAT6-specific inhibitor is not commercially available, we used kaempferol, which inhibits the phosphorylation of STAT6 by JAK3 (28). After an 18-h exposure to *M. pneumoniae* M129, FOXA2 expression was 65% lower than that in cells exposed to PBS (Fig. 8A). In contrast, the expression of FOXA2 was

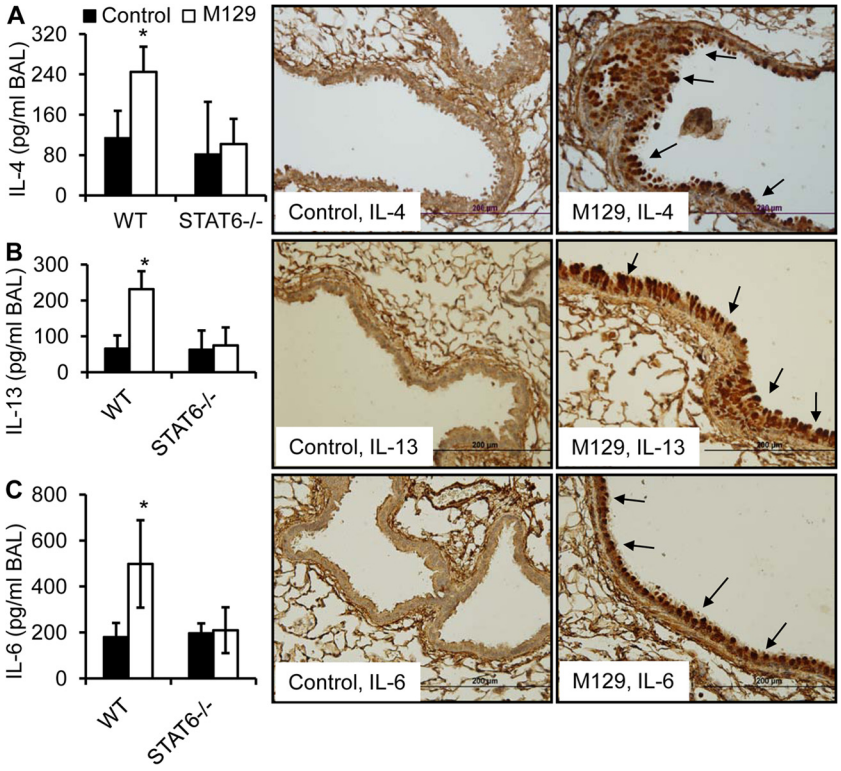

FIG 6 *M. pneumoniae* induces Th2 cytokine expression in mouse lungs. After 3 days of infection with 1×10^8 CFU of *M. pneumoniae* M129, the lungs of C57BL/6 or Stat6$^{-/-}$ mice were sampled by collection of BAL fluid for cytokine determination. IL-4 (A), IL-13 (B), and IL-6 (C) were detected by ELISA ($n = 10$), as well as by IHC staining ($n = 5$) with anti-IL-4, anti-IL-13, and anti-IL-6 antibodies. *, $P < 0.05$ for comparison of the cytokine levels of *M. pneumoniae*-infected samples with those of PBS controls. The statistical significance of differences between samples was determined with the parametric Student *t* test. WT, wild type.

significantly restored when NCI-H292 cells were treated with kaempferol, AG1478, or Cpd188, respectively (Fig. 8A). Treatment with inhibitors of STAT3, STAT6, or EGFR alone did not negatively affect the expression of FOXA2 in the absence of infection with *M. pneumoniae* M129 (see Fig. S1 in the supplemental material). To confirm the results described above, we examined the expression of FOXA2 in NCI-H292 cells infected with *M. pneumoniae* M129 in the presence or absence of gene silencing by EGFR, STAT3, and STAT6 siRNAs. Control NCI-H292 cells that were exposed to a random, nontargeting siRNA sequence showed 40% lower expression of FOXA2 (Fig. 8B, lane 2). In the absence of infection with *M. pneumoniae* M129, silencing of EGFR, STAT3, and STAT6 by individual siRNAs in NCI-H292 cells increased the expression of FOXA2 (Fig. 8B, lanes 3, 5, and 7). Even in the presence of *M. pneumoniae* M129 infection, inhibition of EGFR, STAT3, and STAT6 by siRNA maintained significantly higher levels of FOXA2 expression than in infected NCI-H292 cells treated with the random, nontargeting control siRNA sequence (Fig. 8B, compare lanes 4, 6, and 8 with lane 2). Importantly, Cpd188 also decreased the phosphorylation of STAT6, suggesting that STAT3 acts upstream of STAT6 during the suppression of FOXA2 (Fig. 8C). Collectively, the data presented in Fig. 5 to 8 indicate that *M. pneumoniae* infection activates STAT3, STAT6, and EGFR, which in turn suppresses FOXA2 expression and derepresses MUC5AC and MUC5B expression.

Restoration of FOXA2 expression by STAT3, STAT6, and EGFR inhibitors suppresses mucin overexpression induced by *M. pneumonia*. Next we examined whether restoration of FOXA2 expression by kaempferol, AG1478, and Cpd188 could, in turn, suppress the induction of mucin overexpression mediated by *M. pneumoniae*. Exposure to *M. pneumoniae* M129 stimulated the expression of MUC5AC and MUC5B in NCI-H292 cells 2.9- and 3-fold, respectively (Fig. 9A and B). Importantly, CpD188, kaempferol, and AG1478 attenuated the induction of MUC5AC and MUC5B by *M. pneumoniae* M129 (Fig. 9A and B). These results suggest that EGFR and STAT3-STAT6 signaling pathways play prominent roles during the induction of mucin overexpression by *M. pneumoniae* infection.

DISCUSSION

M. pneumoniae is a common cause of respiratory tract infections in children and adults of all ages. Evidence of *M. pneumoniae*'s role in pulmonary diseases, especially asthma and COPD, is accumulating (12, 13). Although respiratory viruses have been shown to induce acute exacerbation of asthma (8, 11), *M. pneumoniae* may also be involved, especially in the context of superinfection with respiratory viruses (8, 13), and is capable of inducing mucin hypersecretion. However, with the exception of CARDS toxin, the virulence factors and host signaling mechanisms that regulate mucus hypersecretion during *M. pneumoniae* infection remain largely undetermined. In the present study, we demonstrated that *M. pneumoniae* induces mucin overproduction by activating both the STAT3-STAT6 and EGFR signaling pathways, resulting in inhibition of the expression of FOXA2, a major transcriptional repressor of GCHM and mucin biosynthesis. Our conclusions are supported by several lines of experimental evidence. (i) Inhibition

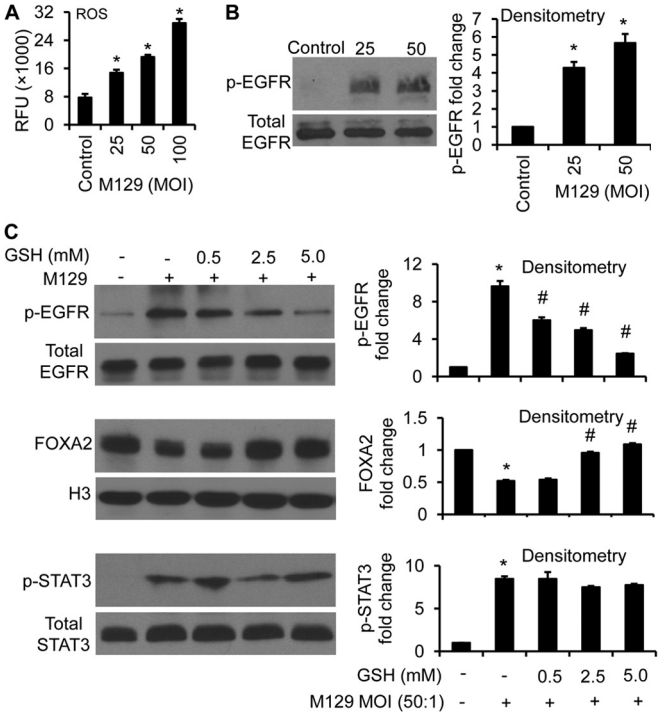

FIG 7 *M. pneumoniae* infection is accompanied by elevated levels of ROS and activation of EGFR. (A) ROS levels in NCI-H292 cells infected with *M. pneumoniae* M129. Experiments were performed in triplicate three times with similar results. The mean values ± the standard deviations of one typical experiment are shown. (B) Phosphorylated EGFR was detected in NCI-H292 cells with an anti-phospho-EGFR antibody 18 h postinfection with *M. pneumoniae* M129. The Western blotting experiments were repeated three times with similar results. (C) GSH attenuates EGFR signaling and restored FOXA2 expression. Densitometry of Western blot assays represents the mean values ± the standard deviations of all three experiments. *, $P < 0.05$ for comparison of *M. pneumoniae*-infected samples with PBS controls with the parametric Student *t* test. #, $P < 0.05$ for comparison of the levels of p-EGFR, FOXA2, and p-STAT3 in *M. pneumoniae*-infected, GSH-treated NCI-H292 cells with those in NCI-H292 cells only infected with *M. pneumoniae* by one-way ANOVA. RFU, relative fluorescence units.

of FOXA2 expression is associated with increased expression of MUC5AC and MUC5B in NCI-H292 cells and ALI cultures of NHBE cells and mouse airways infected with *M. pneumoniae*. (ii) Activated forms of STAT3, STAT6, and EGFR directly associated with FOXA2 inhibition increased in NCI-H292 cells infected with *M. pneumoniae*. (iii) The upstream STAT3 and STAT6 stimuli IL-6, IL-13, and IL-4 were elevated in mouse airways exposed to *M. pneumoniae*, whereas the level of ROS, which activates EGFR, increased in NCI-H292 cells exposed to *M. pneumoniae*. (iv) STAT3, STAT6, and EGFR inhibitors abolished the repression of FOXA2 and mucin overproduction mediated by *M. pneumoniae*. Our study links *M. pneumoniae* infection with the induction and modulation of cellular signaling mechanisms that regulate mucin overexpression.

The regulatory roles of FOXA2 in GCHM and mucin production have only become known in recent years. FOXA2 is expressed in the foregut endoderm and in subsets of respiratory epithelial cells in fetal and adult lungs and regulates several genes that play important roles in lung morphogenesis and homeostasis, including Titf1, Sftpb, and Scgblal (19, 29–32). Selective deletion of the *Foxa2* gene in the respiratory epithelium causes airspace enlargement, GCHM, excessive mucin production, and increased neutrophilic infiltration (19). The expression of FOXA2 was either decreased or absent in the airways of experimental asthma by ovalbumin sensitization (19, 21) and in lung tissues from patients with a variety of pulmonary diseases (19, 21). In the present study, we showed that *M. pneumoniae* infection severely depletes FOXA2 expression, which is associated with mucin overexpression, suggesting that *M. pneumoniae* may be a contributing factor in FOXA2 depletion, GCHM, and mucus hypersecretion during lung infection.

Virulence components, including the P1 adhesin of the attachment organelle and H_2O_2 produced by *M. pneumoniae*, have been implicated to stimulate the production of pro-GCHM Th2 cytokine IL-4 (33, 34). Th2 cytokines, including IL-4 and IL-13, are major stimuli of GCHM and mucin expression through the STAT6 signaling pathway (3). In transgenic mice overexpressing IL-4 or IL-13, expression of FOXA2 was decreased or absent in airway epithelial cells, suggesting that both of these Th2 cytokines downregulate FOXA2 (19). IL-6 is also able to upregulate mucin secretion, partly through the activation of STAT3 (24). Our studies show that *M. pneumoniae* infection increased the expression of IL-4/IL-13 and IL-6, leading to activation of STAT6 and STAT3, respectively. The expression of IL-6, IL-4, and IL-13 was reduced in the airways of Stat6$^{-/-}$ mice infected with *M. pneumoniae*. These observations were consistent with our previous finding that the lungs of Stat6$^{-/-}$ mice exposed to *P. aeruginosa* pyocyanin had reduced expression of IL-4 and IL-13 (18, 35). There are at least two possible explanations for these observations. (i) IL-4 and IL-13 activate STAT6. In turn, STAT6 binds and activates the transcription of these Th2 cytokine genes in a positive-feedback loop manner (36, 37). (ii) Activated STAT6 also binds and activates the transcription of IL-4/IL-13 receptors, as shown in the case of the gene for IL-13R2 (38). Thus, the loss of STAT6 in Stat6$^{-/-}$ mice may have interrupted the positive-feedback loop required to further amplify the expression of Th2 cytokines, as well as the receptors of these cytokines, which in turn reduced the expression of these inflammatory mediators.

Additional evidence supporting the inhibition of FOXA2 by STAT3 and STAT6 comes from the studies with specific inhibitors and gene-silencing siRNA. Inhibition of STAT6 by kaempferol and the STAT3 inhibitor IX Cpd188 rescued FOXA2 expression and abolished mucin overexpression. Similarly, treatment with both STAT3 and STAT6 siRNAs also derepressed FOXA2 expression. Thus, it is likely that *M. pneumoniae* causes excessive mucin overexpression by activating IL-4/IL-13–STAT6 and IL-6–STAT3 signaling, which downregulate the expression of FOXA2. Activated STAT3 appears to function upstream of STAT6, because STAT3 inhibitor IX Cpd188 prevented the phosphorylation of STAT6 in NCI-H292 cells infected with *M. pneumoniae*. Our finding is consistent with a previous report (24) showing that activated STAT3 regulates the accumulation of Th2 cells and cytokines in a mouse model of dust mite-mediated allergic asthma. Most recently, lipid-associated membrane proteins of *M. pneumoniae* have been shown to activate STAT3 through ROS generation (25). However, although *M. pneumoniae* M129 infection induces ROS formation under our experimental conditions, ROS did not appear to activate STAT3 because GSH treatment did not reduce the activation of the transcription factor. More investigations are needed to understand the interactions between ROS induction and the activa-

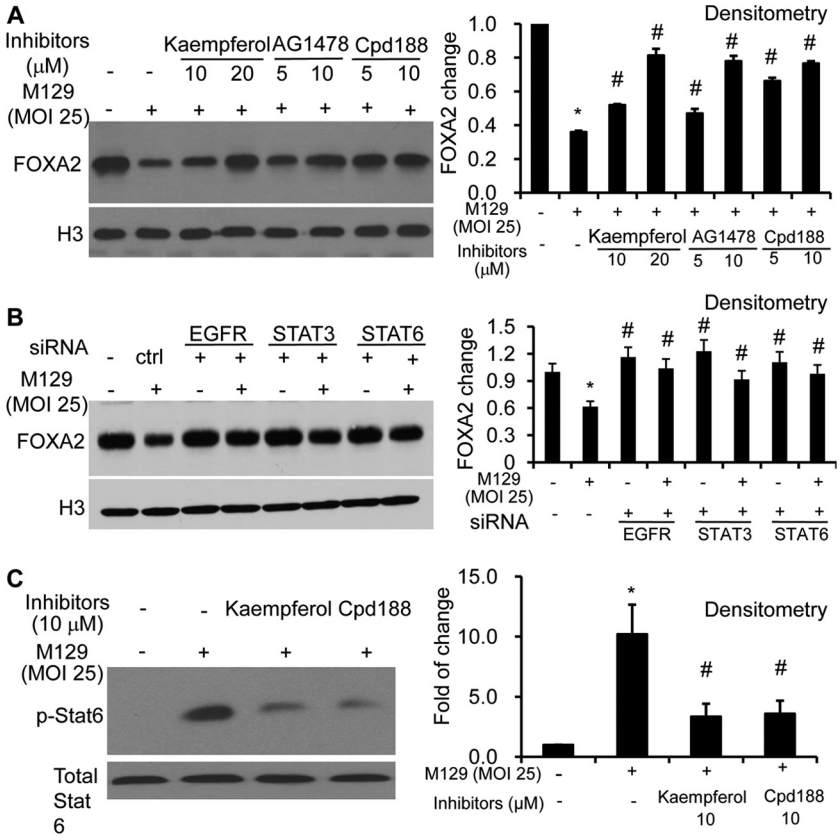

FIG 8 Blockage of the STAT3-STAT6 and EGFR signaling pathways derepresses inhibition of FOXA2 expression by *M. pneumoniae*. (A) Expression of FOXA2 in NCI-H292 cells infected with *M. pneumoniae* M129 in the presence or absence of the STAT6 inhibitor kaempferol, the EGFR inhibitor AG1478, or the STAT3 inhibitor Cpd188. (B) Expression of FOXA2 in NCI-H292 cells infected with *M. pneumoniae* M129 in the presence or absence of gene silencing by EGFR, STAT3, and STAT6 siRNAs. Control (ctrl) NCI-H292 cells (were exposed to a random, nontargeting siRNA sequence. (C) Levels of phosphorylated STAT6 in NCI-H292 cells 18 h after infection with *M. pneumoniae* M129 with or without treatment with kaempferol or Cpd188. Western blotting experiments were repeated three times with similar results. Densitometry of Western blot assays represents the mean values ± the standard deviations from all three experiments. *, $P < 0.05$ for comparison of the levels of FOXA2 in *M. pneumoniae*-infected samples with those in PBS controls by the parametric Student *t* test. #, $P < 0.05$ for comparison of FOXA2 levels in *M. pneumoniae*-infected, inhibitor-treated samples with those in NCI-H292 cells only infected with *M. pneumoniae* by one-way ANOVA.

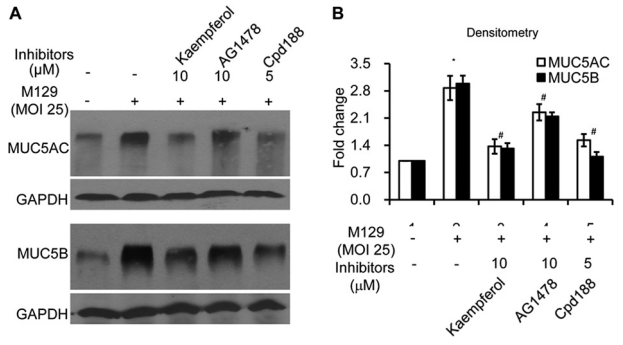

FIG 9 Blockage of the STAT3-STAT6 and EGFR pathways attenuates MUC5AC and MUC5B expression induced by *M. pneumoniae*. (A) Expression of MUC5AC and MUC5B in NCI-H292 cells after 18 h of infection with *M. pneumoniae* M129 in the presence or absence of a STAT6, EGFR, or STAT3 inhibitor. (B) Densitometry analysis of MUC5AC and MUC5B expression in panel A. Western blotting experiments were repeated three times with similar results. Densitometry of Western blot assays represents the mean values ± the standard deviations from all three experiments. *, $P < 0.05$ for comparison of the levels of MUC5AC and MUC5B in *M. pneumoniae*-infected samples with those in PBS controls. #, $P < 0.05$ for comparison of the levels of MUC5AC and MUC5B in *M. pneumoniae*-infected, inhibitor-treated samples with those in NCI-H292 cells only infected with *M. pneumoniae*. The statistical significance of differences between the densitometry values of Western blot assays was determined by one-way ANOVA.

tion of STAT3-STAT6 during *M. pneumoniae* infection-mediated GCHM and mucin hypersecretion.

EGFR is another important modulator of mucin expression (1, 18, 26, 39). Zhen et al. have shown that IL-4/IL-13–STAT6 and EGFR cause GCHM and mucus hypersecretion by independent effects (23). IL-13–STAT6 induces a small set of genes that participate in mucin biosynthesis and modifications. In contrast, EGFR affects numerous genes involved in cell metabolism, survival, transcription, and differentiation. Interestingly, activation of both Stat6 and EGFR inhibits the expression of FOXA2. ROS are the major activators of EGFR signaling during GCHM (26, 39–42). Our data showed high levels of ROS in *M. pneumoniae*-infected NCI-H292 cells, although we did not establish the ROS source. AG1478, an inhibitor of EGFR, as well as the antioxidant GSH, attenuated EGFR activation and restored FOXA2 expression. AG1478 also attenuated mucin expression in *M. pneumoniae*-infected NCI-H292 cells. Finally, it is also possible that ROS produced by *M. pneumoniae* may lead to posttranslational modification and inactivation of FOXA2, as we observed with the redox-active pyocyanin produced by *P. aeruginosa* (20). We are currently examining FOXA2 inactivation by ROS that are released during *M. pneumoniae* infection.

In summary, the present study shows that *M. pneumoniae* causes mucin overproduction by inhibiting the transcriptional repressor FOXA2. This inhibition is mediated through activation of the IL-6–STAT3, IL-4/IL-13–STAT6, and ROS-EGFR signaling pathways. Attenuation of these pro-GCHM pathways and maintenance of FOXA2 function in *M. pneumoniae*-infected airways may improve the lung function of these patients.

ACKNOWLEDGMENTS

This work was supported by the American Lung Association DeSouza Research Award (DS-192835-N) and an NIH grant (HL090699) to G. W. Lau. This investigation was conducted in a facility constructed with support from Research Facilities Improvement Program grant C06 RR 16515-01 from the National Center for Research Resources, National Institutes of Health. The funders had no role in study design, data collection and analysis, the decision to publish, or preparation of the manuscript.

We have no conflict of interest.

REFERENCES

1. **Rose MC, Voynow JA.** 2006. Respiratory tract mucin genes and mucin glycoproteins in health and disease. Physiol. Rev. **86:**245–278. http://dx.doi.org/10.1152/physrev.00010.2005.
2. **Fahy JV, Dickey BF.** 2010. Airway mucus function and dysfunction. N. Engl. J. Med. **363:**2233–2247. http://dx.doi.org/10.1056/NEJMra0910061.
3. **Thornton DJ, Rousseau K, McGuckin MA.** 2008. Structure and function of the polymeric mucins in airways mucus. Annu. Rev. Physiol. **70:**459–486. http://dx.doi.org/10.1146/annurev.physiol.70.113006.100702.
4. **Knowles MR, Boucher RC.** 2002. Mucus clearance as a primary innate defense mechanism for mammalian airways. J. Clin. Invest. **109:**571–577. http://dx.doi.org/10.1172/JCI200215217.
5. **Kuyper LM, Paré PD, Hogg JC, Lambert RK, Ionescu D, Woods R, Bai TR.** 2003. Characterization of airway plugging in fatal asthma. Am. J. Med. **115:**6–11. http://dx.doi.org/10.1016/S0002-9343(03)00241-9.
6. **Hogg JC, Chu F, Utokaparch S, Woods R, Elliott WM, Buzatu L, Cherniack RM, Rogers RM, Sciurba FC, Coxson HO, Paré PD.** 2004. The nature of small-airway obstruction in chronic obstructive pulmonary disease. N. Engl. J. Med. **350:**2645–2653. http://dx.doi.org/10.1056/NEJMoa032158.
7. **Koeppen M, McNamee EN, Brodsky KS, Aherne CM, Faigle M, Downey GP, Colgan SP, Evans CM, Schwartz DA, Eltzschig HK.** 2013. Detrimental role of the airway mucin muc5ac during ventilator-induced lung injury. Mucosal Immunol. **6:**762–775. http://dx.doi.org/10.1038/mi.2012.114.
8. **Wilkinson TM, Hurst JR, Perera WR, Wilks M, Donaldson GC, Wedzicha JA.** 2006. Effect of interactions between lower airway bacterial and rhinoviral infection in exacerbations of COPD. Chest **129:**317–324. http://dx.doi.org/10.1378/chest.129.2.317.
9. **Chu HW, Jeyaseelan S, Rino JG, Voelker DR, Wexler RB, Campbell K, Harbeck RJ, Martin RJ.** 2005. TLR2 signaling is critical for *Mycoplasma pneumoniae*-induced airway mucin expression. J. Immunol. **174:**5713–5719. http://dx.doi.org/10.4049/jimmunol.174.9.5713.
10. **Kraft M, Adler KB, Ingram JL, Crews AL, Atkinson TP, Cairns CB, Krause DC, Chu HW.** 2008. *Mycoplasma pneumoniae* induces airway epithelial cell expression of MUC5AC in asthma. Eur. Respir. J. **31:**43–46. http://dx.doi.org/10.1183/09031936.00103307.
11. **Hashimoto K1, Graham BS, Ho SB, Adler KB, Collins RD, Olson SJ, Zhou W, Suzutani T, Jones PW, Goleniewska K, O'Neal JF, Peebles RS, Jr.** 2004. Respiratory syncytial virus in allergic lung inflammation increases muc5ac and gob-5. Am. J. Respir. Crit. Care Med. **170:**306–312. http://dx.doi.org/10.1164/rccm.200301-030OC.
12. **Waitest KB, Balish MF, Atkinson TP.** 2008. New insights into the pathogenesis and detection of *Mycoplasma pneumoniae* infections. Future Microbiol. **3:**635–648. http://dx.doi.org/10.2217/17460913.3.6.635.
13. **Sutherland ER, Brandorff JM, Martin RJ.** 2004. Atypical bacterial pneumonia and asthma risk. J. Asthma **41:**863–868. http://dx.doi.org/10.1081/JAS-200038477.
14. **Waldo RH, Krause DC.** 2006. Synthesis, stability, and function of cytadhesin p1 and accessory protein B/C complex of *Mycoplasma pneumoniae*. J. Bacteriol. **188:**569–575. http://dx.doi.org/10.1128/JB.188.2.569-575.2006.
15. **Pilo P, Vilei EM, Peterhans E, Bonvin-Klotz L, Stoffel MH, Dobbelaere D, Frey J.** 2005. A metabolic enzyme as a primary virulence factor of *Mycoplasma mycoides* subsp. *mycoides* small colony. J. Bacteriol. **187:**6824–6831. http://dx.doi.org/10.1128/JB.187.19.6824-6831.2005.
16. **Kannan TR, Provenzano D, Wright JR, Baseman JB.** 2005. Identification and characterization of human surfactant protein a binding protein of *Mycoplasma pneumoniae*. Infect. Immun. **73:**2828–2834. http://dx.doi.org/10.1128/IAI.73.5.2828-2834.2005.
17. **Medina JL, Coalson JJ, Brooks EG, Winter VT, Chaparro A, Principe MF, Kannan TR, Baseman JB, Dube PH.** 2012. *Mycoplasma pneumoniae* cards toxin induces pulmonary eosinophilic and lymphocytic inflammation. Am. J. Respir. Cell Mol. Biol. **46:**815–822. http://dx.doi.org/10.1165/rcmb.2011-0135OC.
18. **Hao Y, Kuang Z, Walling BE, Bhatia S, Sivaguru M, Chen Y, Gaskins HR, Lau GW.** 2012. *Pseudomonas aeruginosa* pyocyanin causes airway goblet cell hyperplasia and metaplasia and mucus hypersecretion by inactivating the transcriptional factor foxa2. Cell. Microbiol. **14:**401–415. http://dx.doi.org/10.1111/j.1462-5822.2011.01727.x.
19. **Wan H, Kaestner KH, Ang SL, Ikegami M, Finkelman FD, Stahlman MT, Fulkerson PC, Rothenberg ME, Whitsett JA.** 2004. Foxa2 regulates alveolarization and goblet cell hyperplasia. Development **131:**953–964. http://dx.doi.org/10.1242/dev.00966.
20. **Hao Y, Kuang Z, Xu Y, Walling BE, Lau GW.** 2013. Pyocyanin-induced mucin production is associated with redox modification of FOXA2. Respir. Res. **14:**82. http://dx.doi.org/10.1186/1465-9921-14-82.
21. **Park SW, Verhaeghe C, Nguyenvu LT, Barbeau R, Eisley CJ, Nakagami Y, Huang X, Woodruff PG, Fahy JV, Erle DJ.** 2009. Distinct roles of FOXA2 and FOXA3 in allergic airway disease and asthma. Am. J. Respir. Crit. Care Med. **180:**603–610. http://dx.doi.org/10.1164/rccm.200811-1768OC.
22. **Morton HE, Smith PF, Leberman PR.** 1951. Investigation of the cultivation of pleuropneumonia-like organisms from man. Am. J. Syph. Gonorrhea Vener. Dis. **35:**361–369.
23. **Zhen G, Park SW, Nguyenvu LT, Rodriguez MW, Barbeau R, Paquet AC, Erle DJ.** 2007. IL-13 and epidermal growth factor receptor have critical but distinct roles in epithelial cell mucin production. Am. J. Respir. Cell Mol. Biol. **36:**244–253. http://dx.doi.org/10.1165/rcmb.2006-0180OC.
24. **Simeone-Penney MC, Severgnini M, Tu P, Homer RJ, Mariani TJ, Cohn L, Simon AR.** 2007. Airway epithelial STAT3 is required for allergic inflammation in a murine model of asthma. J. Immunol. **178:**6191–6199. http://dx.doi.org/10.4049/jimmunol.178.10.6191.
25. **Choi SY, Lim JW, Shimizu T, Kuwano K, Kim JM, Kim H.** 2012. Reactive oxygen species mediate JAK2/STAT3 activation and IL-8 expression in pulmonary epithelial cells stimulated with lipid-associated membrane proteins from *Mycoplasma pneumoniae*. Inflamm. Res. **61:**493–501. http://dx.doi.org/10.1007/s00011-012-0437-7.
26. **Takeyama K, Fahy JV, Nadel JA.** 2001. Relationship of epidermal growth factor receptors to goblet cell production in human bronchi. Am. J. Respir. Crit. Care Med. **163:**511–516. http://dx.doi.org/10.1164/ajrccm.163.2.2001038.
27. **Sun G, Xu X, Wang Y, Shen X, Chen Z, Yang J.** 2008. *Mycoplasma pneumoniae* infection induces reactive oxygen species and DNA damage in A549 human lung carcinoma cells. Infect. Immun. **76:**4405–4413. http://dx.doi.org/10.1128/IAI.00575-08.
28. **Cortes JR, Perez-G M, Rivas MD, Zamorano J.** 2007. Kaempferol inhibits IL-4-induced STAT6 activation by specifically targeting JAK3. J. Immunol. **179:**3881–3887. http://dx.doi.org/10.4049/jimmunol.179.6.3881.
29. **Costa RH, Kalinichenko VV, Lim L.** 2001. Transcription factors in mouse lung development and function. Am. J. Physiol. Lung Cell. Mol. Physiol. **280:**L823–L838.
30. **Ikeda K, Shaw-White JR, Wert SE, Whitsett JA.** 1996. Hepatocyte nuclear factor 3 activates transcription of thyroid transcription factor 1 in respiratory epithelial cells. Mol. Cell. Biol. **16:**3626–3636.
31. **Bohinski RJ, Dilauro R, Whitsett JA.** 1994. The lung-specific surfactant protein B gene promoter is a target for thyroid transcription factor 1 and hepatocyte nuclear factor 3, indicating common factors for organ-specific gene expression along the foregut axis. Mol. Cell. Biol. **14:**5671–5681. http://dx.doi.org/10.1128/MCB.14.9.5671.
32. **Bingle CD, Hackett BP, Moxley M, Longmore W, Gitlin JD.** 1995. Role of hepatocyte nuclear factor-3 alpha and hepatocyte nuclear factor-3 beta

in Clara cell secretory protein gene expression in the bronchiolar epithelium. Biochem. J. **308:**197–202.
33. **Hoek KL, Duffy LB, Cassell GH, Dai Y, Atkinson TP.** 2005. A role for the *Mycoplasma pneumoniae* adhesin p1 in interleukin (IL)-4 synthesis and release from rodent mast cells. Microb. Pathog. **39:**149–158. http://dx.doi.org/10.1016/j.micpath.2005.07.004.
34. **Atkinson TP, Dai Y, Duffy LB.** 2007. Role of hydrogen peroxide in *Mycoplasma pneumoniae*-induced mast cell IL-4 production. J. Allergy Clin. Immun. **119:**S54–S54. http://dx.doi.org/10.1016/j.jaci.2006.11.235.
35. **Caldwell CC, Chen Y, Borchers MT, Goetzmann H, Hassett DJ, Young LR, Mavrodi D, Thomashow L, Lau GW.** 2009. *Pseudomonas aeruginosa* pyocyanin causes cystic fibrosis airway pathogenesis. Am. J. Pathol. **175:**2473–2488. http://dx.doi.org/10.2353/ajpath.2009.090166.
36. **Kubo M, Ransom J, Webb D, Hashimoto Y, Tada T, Nakayama T.** 1997. T cell subset-specific expression of the IL-4 gene is regulated by a silencer element and STAT6. EMBO J. **16:**4007–4020. http://dx.doi.org/10.1093/emboj/16.13.4007.
37. **Curiel RE, Lahesmaa R, Subleski J, Cippitelli M, Kirken RA, Young HA, Ghosh P.** 1997. Identification of a Stat-6-responsive element in the promoter of the human interleukin-4 gene. Eur. J. Immunol. **27:**1982–7198. http://dx.doi.org/10.1002/eji.1830270823.
38. **David MD, Bertoglio J, Pierre J.** 2003. Functional characterization of IL-13 receptor alpha2 gene promoter: a critical role of the transcription factor STAT6 for regulated expression. Oncogene **22:**3386–3394. http://dx.doi.org/10.1038/sj.onc.1206352.
39. **Rada B, Gardina P, Myers TG, Leto TL.** 2011. Reactive oxygen species mediate inflammatory cytokine release and EGFR-dependent mucin secretion in airway epithelial cells exposed to *Pseudomonas* pyocyanin. Mucosal Immunol. **4:**158–171. http://dx.doi.org/10.1038/mi.2010.62.
40. **Yang J, Li Q, Zhou XD, Kolosov VP, Perelman JM.** 2011. Naringenin attenuates mucous hypersecretion by modulating reactive oxygen species production and inhibiting NF-κB activity via EGFR-PI3K-Akt/ERK MAPKinase signaling in human airway epithelial cells. Mol. Cell. Biochem. **351:**29–40. http://dx.doi.org/10.1007/s11010-010-0708-y.
41. **Casalino-Matsuda SM, Monzon ME, Forteza RM.** 2006. Epidermal growth factor receptor activation by epidermal growth factor mediates oxidant-induced goblet cell metaplasia in human airway epithelium. Am. J. Respir. Cell Mol. Biol. **34:**581–591. http://dx.doi.org/10.1165/rcmb.2005-0386OC.
42. **Yu H, Zhou X, Wen S, Xiao Q.** 2012. Flagellin/TLR5 responses induce mucus hypersecretion by activating EGFR via an epithelial cell signaling cascades. Exp. Cell Res. **318:**723–731. http://dx.doi.org/10.1016/j.yexcr.2011.12.016.